Fenollosa Esteve, R.; Ramiro-Manzano, F.; Garín Escrivá, M.; Alcubilla, R. (2019). Thermal Emission of Silicon at Near-Infrared Frequencies Mediated by Mie Resonances. ACS Photonics. 6(12):3174-3179. https://doi.org/10.1021/acsphotonics.9b01513

Thermal Emission of Silicon at Near Infrared Frequencies Mediated by Mie Resonances

Roberto Fenollosa,[*,†] Fernando Ramiro-Manzano,[†] Moisés Garín,[‡,§] and Ramón Alcubilla[§]*

[†]Instituto Universitario de Tecnología Química, CSIC-UPV, Universitat Politècnica de València, Av. dels Tarongers, València 46022, Spain

[‡]GR-MECAMAT, Universitat de Vic – Universitat Central de Catalunya (UVIC-UCC), Campus Torre dels Frares, c/ de la Laura 13, 08500 Vic, Spain.

[§]Departament d'Enginyeria Electrònica, Universitat Politècnica de Catalunya, Jordi Girona 1-3, Barcelona 08034, Spain

PACS numbers: 44.40.+a, 42.60.Da, 42.72.Ai, 78.20.Bh

*E-mail: rfenollo@ter.upv.es

Keywords: microsphere, silicon, nanocavity, whispering gallery modes, super-Planckian, light source

Abstract

Planck's law constitutes one of the cornerstones in physics. It explains the well-known spectrum of an ideal black body consisting of a smooth curve, whose peak wavelength and intensity depend on the temperature of the body. This scenario changes drastically, however, when the size of the emitting object is comparable to the wavelength of the emitted radiation. Here we show that a silicon micro-sphere (2-3 μm in diameter) heated to around 800 ºC yields a thermal emission spectrum consisting of pronounced peaks that are associated with Mie resonances. We experimentally demonstrate in the near infrared the existence of modes with an ultra-high quality factor, Q, of 400, which is substantially higher than values reported so far, and set a new benchmark in the field of thermal emission. Simulations predict that the thermal response of the micro-spheres is very fast, about 15 μs. Additionally, the possibility of achieving light emission above the Planck limit at some frequency ranges is envisaged.

Nanotechnology has been proven to be a determining tool for testing the limits of fundamental physical laws. When the size of a thermal radiation emitter or the distance between emitter and receiver decreases below λ_{rad}, which is the wavelength at which emission intensity is maximum for a given temperature (Wien displacement law),[1] interesting effects appear. One prominent phenomenon is the emission above the Planck limit,[2, 3] which has been measured in the near [4] and in the far field[5] regimes. However, so far there have been few experiments in this regard, and they are usually based on structures where only one or two dimensions are smaller than λ_{rad}. One of the challenges here is the detection of the low radiation intensities produced by such small bodies.[6, 7, 8] The experiments that we report in this article are framed in a scenario where the size of the emitter, a silicon micro-sphere, is comparable or smaller than λ_{rad} in the three dimensions of space, and result in emission spectra with substantial deviations from that of a black body.

Besides fundamental physics, another important facet of our experiments concerns technological aspects regarding the engineering of light sources.[9, 10] In recent years, tailoring of different aspects of the radiated light: wavelength, directionality, coherence and efficiency, was achieved by structuring materials as photonic crystals[11-15] (*PC*), optical antennas,[8, 16] metamaterials[17, 18] and cavities.[19, 20]

In general, and particularly for some applications such as non-dispersive infrared sensing,[21, 22] it is interesting to engineer light sources with a peaked emission and a fast response. In this context, very relevant achievements based on 2D *PC* devices were recently reported.[23] Single peak emissions with Q about 100 and dynamic control of the emitted light at 600 kHz were demonstrated in the mid infrared (MIR) by modulating the emissivity of the device rather than its temperature, which remained constant at a relatively low value. In this case, the requirement of establishing electrical contacts on the device may hinder the possibility of

achieving higher working temperatures, which would allow higher light intensities and emission more towards the NIR to be accomplished. Therefore, there is still much room for improvement and for innovative approaches in this field of technology.

The resonant thermal light emission characteristics of wavelength-sized silicon spheres[24] that we report here stem from the fact that they constitute high refractive index contrast photonic micro-cavities. Silicon is in principle not suitable for emitting light in the NIR at room temperature (*RT*) because it is transparent in this region, and according to Kirchhoff's law[25] the emissivity of a material equals the absorptivity at a given frequency. However, this scenario changes completely as the temperature of the material increases, because it produces a change in its electronic properties, namely a redshift of the indirect band gap (located at 1.125 μm at *RT*), and an increase in the density of free carriers (*FC*). The resultant effect of these phenomena is an increase of both the real part, n (thermo-optic effect, *TOE*), and the imaginary part, k, of the refractive index. While the *TOE* shifts the spectral position of the resonant modes, the change in k determines which of them are going to prevail in an absorption (or emission) process.[26] Low k values require relatively low temperatures and they would allow light emission through high Q resonances. However, because of Stefan and Wien laws,[1] the emitted power would be in principle too low to be detected and the wavelength at which the maximum of radiation occurs is far from the NIR. On the other hand, a high increase of temperature and thus of k above the Q matching condition[26] is expected to kill any resonant mode, although it would yield high radiation intensities. We have found, within these two extreme regimes, a range of temperatures: from 700 ºC to 850 ºC approximately where reasonable emission occurs in the NIR through moderate, yet very high for thermal radiation, Q resonances.

Previously reported measurements of light emission assisted by Mie resonances were performed in metal oxide particles suspended in an optical trap at temperatures near the melting point of the material.[27] In our approach, however, a silicon micro-sphere is located on a SiO_2 substrate (Figure 1a) and it is heated at moderate temperatures. This contributes to improve its handling and stability. Moreover, the reduced size of the emitting cavity makes it suitable for exploring its performance as a broadband micro-scale light or heat source,[28] able to transfer energy to other objects closely placed. In fact, the use of resonant dielectric nanoparticles based on silicon has already been explored to develop an efficient temperature feedback optical heating platform.[29] Our approach embodies an alternative strategy, amongst the different approaches undertaken so far, which concerns that eagerly pursued dream of obtaining light emission from silicon,[30, 31] the king material for micro-electronics. In this sense, a more on-chip fabrication methodology[32] could help to further develop this application in the future.

The mechanism we have utilized here for heating a silicon micro-sphere is based on the capacity of the material for absorbing light above the band gap. For that purpose, we focused the light at 405 nm of a laser (pumping laser from now on) on top of the micro-sphere (Figure 1a). The geometry of our approach where a high heat conducting micro-sphere [the thermal conductivity, κ, equals to 130 W/(m K) for Si] is supported and surrounded by low heat conductors: SiO_2 [κ = 1.38 W/(m K)] and air [κ = 0.024 W/(m K)], favors the efficiency of the heating process. In this regard, a power of 5 mW approximately from the pumping laser was needed for achieving the aforementioned temperatures.

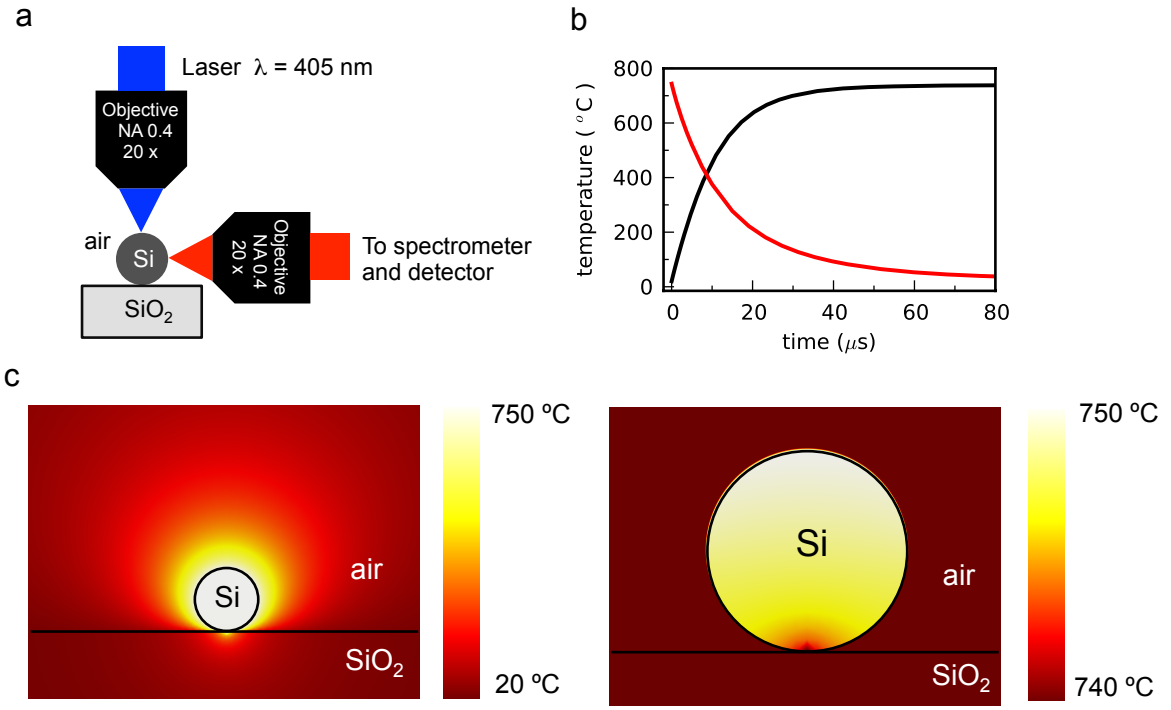

Figure 1. Experimental set up and FEM simulation of the temperature distribution and time response of the heating process of a silicon micro-sphere from room temperature to 750 ºC. (a) Schematic of the set up utilized for the experiments, showing how a silicon micro-sphere supported on a SiO_2 substrate in air is heated by a blue laser and the thermal emission spectrum is collected at a plane parallel to the substrate. (b) Heating (black curve) and cooling (red curve) time evolution of the average temperature of the micro-sphere upon starting and stopping respectively the irradiation with the blue laser. (c) Cross section view at different scales of the temperature distribution at steady state condition.

According to Finite Element Method (FEM) simulations, and as expected because of its low mass, which is of the order of tens of picograms, the micro-spheres temperature response upon irradiation by the laser is very fast (Figure 1b). The heating process (black curve) takes about 10 μs, while the cooling time is slightly longer, 15 μs for a 3.5 μm diameter micro-sphere (see Methods section). This implies the possibility of reaching radiation modulation

frequencies of 10 kHz, which are much faster than the conventional temperature modulations, in the range from 10 to 100 Hz, reached so far.[22]

The simulations reveal that in spite of the low thermal conductivity of the materials surrounding the micro-sphere, the heat release via conduction is three orders of magnitude higher than that via radiation. Nevertheless, the energy loss by conduction could be reduced in vacuum conditions, although at the expense of an increase in the response time, especially the cooling time. In terms of thermal conductivity, the substrate constitutes the main heat sink and it produces a thermal asymmetry in the vertical direction, namely a temperature gradient of about 10 ºC from top to bottom (Figure 1c). The pumping laser also contributes to this asymmetry but to a much lesser extend because of the high thermal conductivity of silicon. On the other hand, the temperature through planes parallel to the substrate was found to be uniform. This is very relevant with respect to our measurements because we collected only light emitted tangentially to the sphere at that resonant plane which is parallel to the substrate (Figure 1a), although emission occurs in all directions of space. The collection configuration is similar to that utilized for scattering experiments[33] and it helps disregarding non-resonant emission, those not so pure modes occurring at different zenith angles, whose resonant planes intersect the substrate,[34] and that radiation originated at a temperature different from that of the equatorial plane.

The measured steady state thermal emission spectra at near infrared frequencies are shown in Figure 2a,b (black curves in right panels), for two different micro-spheres. A fitting process (see Methods section and Supporting Information) was undertaken using the Planck equation[35] for the emissive power, I, of radiation of a black body, modulated by the absorption efficiency, Q_{abs}, that works as the emissivity parameter for a micro-sphere[36] [Equation (1)].

$$I = \frac{2\pi hc^2}{\lambda^5 e^{\left(\frac{hc}{\lambda kT}-1\right)}} Q_{abs} \quad (1)$$

The sphere diameter (Φ), which is required for calculating Q_{abs} from Mie theory[37] was deduced previously from optical scattering measurements at room temperature.[33] Therefore, the main fitting parameters are the temperature, T, at which the emission occurs, and a second ingredient, that will be explained below, consisting of the density of free carriers associated to the pumping laser (n_{FCL}). Q_{abs} depends on the refractive index dispersion, which in turn depends on the temperature. We obtained the relation between refractive index and temperature from the literature.[38, 39] Theoretical spectra (red curves) yield a fairly good agreement with experiment for those fitted parameters summarized in Table 1. Each peak of the spectra corresponds to a Mie resonance. They have been indicated by letters for each micro-sphere and identified in Table 2. Other micro-spheres thermal emission at different temperatures are shown in the Supporting Information.

Based on the FEM calculations that indicate the temperature is uniform in planes parallel to the substrate, and on our measurement conditions mentioned above (Fig. 1), we assumed a theoretical model where the temperature is considered uniform in all the sphere volume.[36] In fact, the calculations reveal that the temperature variation within the volume occupied by a typical resonance is around 1ºC (see Supporting Information). The success of the fit process in a wide wavelength range reinforces this assumption. However, we should beware of the limitations of this model and of what the fitted temperature represents, i.e. the temperature of the micro-sphere at the equatorial plane parallel to the substrate. Although it is beyond the scope of this article, a more detailed theory based on fluctuational electrodynamics[40] that takes into account the actual temperature profile would be convenient to better explain the experimental results.

Table 1. Main fitted parameters for the emission spectra of Figure 2a,b.

Fig.	Φ (nm)	t (ºC)	n_{FCL} (cm^{-3})
2a	3595 ± 5	756 ± 1	$(3.6 \pm 0.9)x10^{18}$
2b	2308 ± 5	841 ± 1	$(3.0 \pm 0.2)x10^{18}$

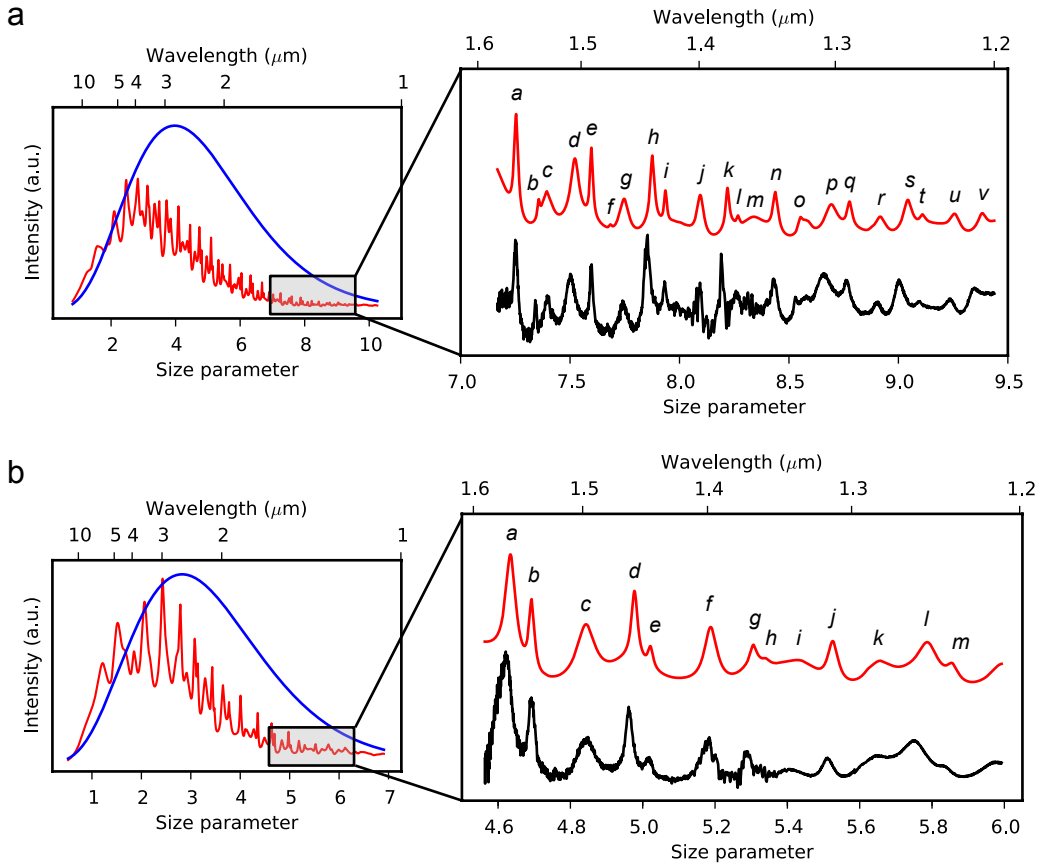

Figure 2. Thermal emission spectra of silicon micro-spheres (a) Measured spectrum in the NIR for a 3595 nm diameter (Φ) silicon micro-sphere (black curve in right panel). It agrees with that spectrum obtained from fitting the experimental data to Eq. (1) (red curve) with a fitted temperature of 756 ºC (see Table 1). The calculation indicates that the emission occurs in a much wider range of wavelengths towards the MIR (left panel) and it can reach intensities above the Planck limit (blue curve) at some frequency ranges. The spectra have been plotted against size parameter, defined as (π Φ/λ), and wavelength. (b) The same as (a) but for a 2308 nm diameter silicon micro-sphere with a fitted temperature of 841 ºC.

Table 2. Transverse Electric (TE) and Transverse Magnetic (TM) Mie modes associated to the spectral peaks of Figure 2 a,b.

Peak	Fig. 2a	Fig. 2b
a	$TE_{9,5}$	$TM_{6,3}$
b	$TM_{11,4}$	$TE_{7,3}$
c	$TE_{12,4}$	$TE_{5,4}$
d	$TM_{9,5}$	$TM_{7,3}$
e	$TE_{10,5}$	$TE_{8,3}$
f	$TM_{12,4}$	$TE_{6,4}$
g	$TE_{8,6}$	$TM_{8,3}$
h	$TM_{10,5}$	$TE_{9,3}$
i	$TE_{11,5}$	$TM_{6,4}$
j	$TE_{9,6}$	$TE_{7,4}$
k	$TM_{11,5}$	$TE_{5,5}$
l	$TE_{12,5}$	$TM_{7,4}$
m	$TM_{9,6}$	$TE_{8,4}$
n	$TE_{10,6}$	
o	$TM_{12,5}$	
p	$TM_{10,6}$	
q	$TE_{11,6}$	
r	$TE_{9,7}$	
s	$TM_{11,6}$	
t	$TE_{12,6}$	
u	$TE_{10,7}$	
v	$TM_{12,6}$	

Although the measurements are constrained to the NIR range because of the limitations of our optical setup, it should be stressed that Mie resonant emission also occurs at longer wavelengths according to the theory, in the MIR within our working range of temperatures (red curves in left panels). The intensity of the resonances can reach higher values there because the maximum for the pure black body emission spectra (blue curves) is located around 3 μm [see Equation (1)]. Moreover, emission intensities above the Planck limit[2, 3] are envisaged at some spectral positions, towards long wavelengths, where Q_{abs} reaches values greater than 1. This means that a silicon micro-sphere would emit more light at those wavelengths than a black body having an area equal to that obtained from the geometrical projection of the micro-sphere.[26, 37]

The approach we are reporting here allows tuning different aspects of the emission spectra. The distance between adjacent modes, which is known as free spectral range (*FSR*), can be adjusted by choosing the size of the micro-sphere. The smaller the micro-sphere, the larger the *FSR* is. This can be verified by comparing the spectrum of Figure 2a, with that of Figure 2b, which correspond to average *FSR's* of about 70 and 100 nm respectively around 1.5 μm. On the other hand, the size of the micro-sphere influences the *Q* of emission peaks as well, with higher *Q's* attainable in general as the sphere diameter increases. In the case of the micro-sphere of figure 2a, the typical Mie resonances favoured at 756 ºC show *Q*'s of several hundred around 1.5 μm. Their electric field intensity profile at the resonant plane consists of several maximums through the sphere perimeter and in the radial direction. Figure 3 indicates that the *k* values are of the order of 10^{-3} around that wavelength (green curve). The *k* increase of one order of magnitude at shorter wavelengths smears out all the resonant peaks at that spectral region. The figure also shows the total absorption coefficient (black curve) from which the *k* values were calculated, and the position of the band gap, E_g, at 1.452 μm for 756 ºC. The total absorption coefficient has two main contributions: band gap (blue curve) and *FC* [39] (red curve). We have neglected the lattice absorption because it occurs at wavelengths longer than 6 μm approximately, and it is much lower than the *FC* term at the temperatures of our experiments.[41] The temperature is, in principle, the most determinant factor for *FC* generation. However, the pumping laser at 405 nm is expected to produce additional *FC* at the same time. The fit process yielded, in fact, a density of *FC* produced by the pumping laser [$(3.6 \pm 0.9) \times 10^{18}$ cm^{-3}], higher than that associated with the temperature (1.9×10^{18} cm^{-3}). Nevertheless, a contribution from impurities ionization, whose quantification is beyond our capabilities, should not be disregarded. For comparison, the absorption produced only by temperature generated *FC* is shown as a dashed red curve in the figure.

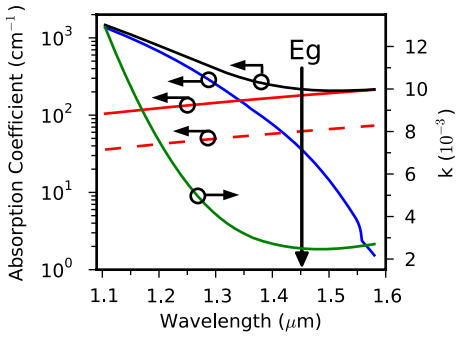

Figure 3. Optical absorption parameters for silicon at high temperature. The green curve corresponds to the imaginary part of the refractive index at 756 ºC, the temperature of the measurement of figure 2a. It was obtained from the total absorption coefficient (black curve), which has two main contributions: band gap (blue curve) and free carriers (red curve) that are originated by the temperature and by the pumping laser. For comparison, the dashed red curve shows the absorption produced by the free carriers associated only to temperature. The position of the band gap, E_g, at 756 ºC is indicated.

Finally, another interesting aspect of the system to underline is the possibility of easily tuning the spectral position of the resonant peaks by taking advantage of the *TOE* effect. This is demonstrated in figure 4a for mode *e* ($TE_{10,5}$) of figure 2a. Its electric field intensity profile at the resonance plane is depicted in figure 4b. The rise of temperature from 756 ºC (red dots) to 792 ºC (black dots), that we realized by slightly increasing the power of the pumping laser, produced a red shift of about 5 nm. A Lorentzian fit of the peaks (continuous lines) yielded a Q of 400 ± 40 in both cases. According to the theory, however, they could be improved to nearly 1000 by preventing the additional *FC* of the pumping laser from being present (see Supporting Information). This could be achieved by using other heating methods.

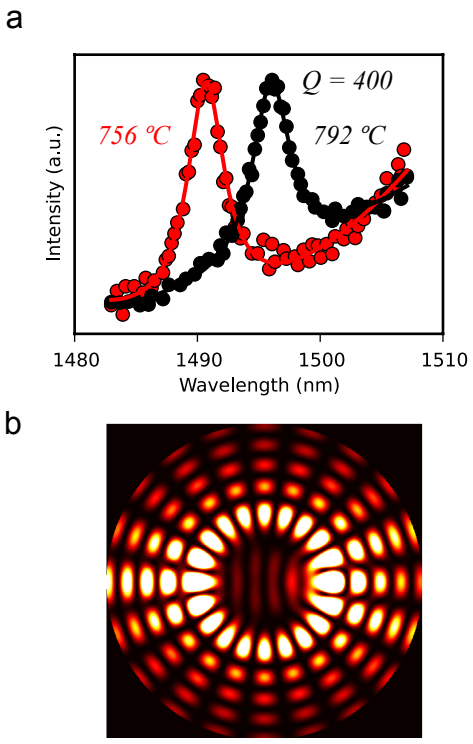

Figure 4. Demonstration of a resonance tuning by temperature and its high Q. (a) Measured resonance $TE_{10,5}$ of micro-sphere of figure 2a at 756 ºC (red dots) and at 792 ºC (black dots). The continuous curves correspond to Lorentzian fits that yield a Q of 400 ± 40 in both cases. (b) Electric field intensity distribution of the mode at the resonance plane.

In conclusion, we have shown a wavelength-sized platform based on silicon for obtaining resonant light at relevant spectral regions such as those of the telecommunication windows, and for studying fundamental aspects of physics related to thermal radiation. It presents a very promising scenario for silicon micro-spheres in the near future.

Methods

Synthesis and processing of the material. Silicon micro-spheres were synthesized by means of a Chemical Vapour Deposition process and they were submitted to a slow crystallization treatment[33] at 800 ºC. The as-grown samples consist of silicon substrates containing many micro-spheres separated from each other. Some of them were transferred by micro-manipulation means to SiO_2 substrates for measuring their thermal emission spectra.

Measurement of the thermal light emission. An iHR 320 Horiba spectrometer with a liquid nitrogen refrigerated InGaAs linear array detector was used for measuring the spectra of the thermal light emitted by silicon micro-spheres. The entrance slit of the spectrometer was set to 0.1 mm and the signals were integrated over 15 s. The as-measured emission spectra were baseline corrected in order to remove the influence of the sensitivity of the optical system produced by mirrors, diffraction gratings, etc, and of any spurious signal that could obscure the resonant peaks. Additionally, before and after each thermal emission measurement, scattering spectra[33] at room temperature were recorded in order to check the condition of the micro-sphere. No changes were observed in this regard as long as the temperature did not surpass 800 ºC. Above this temperature, however, non-reversible changes consisting of small blue shifts of several nm in the resonances position occurred. We think that this can be produced by further changes in the crystal domains, and thus in the sphere diameter, provoked when exceeding the crystallization temperature at which the micro-spheres had been submitted. Moreover, oxidation processes could produce noticeable structural changes as the temperature increases at such high values.[42]

FEM Simulations. Comsol Multiphysics was used for Finite Element Method (FEM) simulations. We took into account conduction and radiation as the heat transfer mechanisms. The characteristic heating response time in Figure 1b is that time where the temperature of the micro-sphere equals to $(T_{max} - T_{RT}) \times (1 - e^{-1})$, where T_{max} is the maximum temperature at

steady state condition, and T_{RT} is room temperature. The cooling time corresponds to that time for which the temperature decreases to T_{max} x e^{-1} from its maximum value. Both equations correspond to the charge and discharge times respectively of the capacitive element in an equivalent *RC* electrical circuit. The maximum modulation frequency is determined by the cooling process, which takes a bit longer than the heating process.

Fits. The measured spectra of figure 2 a,b were fitted to equation (1) plus a quadratic baseline and a normalization factor by Weighted Orthogonal Distance Regression (see Supporting Information for a more detailed description). The peaks of figure 4 were fitted to a Lorentzian function plus a quadratic baseline by the method of Least Squares. In all the cases the errors obtained for the fitted parameters come from the covariance matrix resulting from the fitting process.

Supporting Information

(S1) Fitting process of the black body emission spectrum of a silicon micro-sphere; (S2) Back body emission spectra of the micro-sphere of Figure 2a at three different temperatures; (S3) Emission spectra of other Si microspheres; (S4) Thermal profile and photonic resonance overlap

Corresponding Author

*E-mail: rfenollo@ter.upv.es

Author Contributions

R. F. synthesized and processed silicon micro-spheres, developed the optical setup, performed the experiments and simulations, and wrote the manuscript. F. R. supervised FEM simulations and assisted in the development of the optical setup. M. G. and R. A. assisted in the synthesis of silicon micro-spheres and in the development of the optical setup. All authors discussed and revised the manuscript.

Acknowledgements

This work was supported by several projects of the Spanish Ministry of Economy and Competitiveness (MIMECO): Severo Ochoa program for Centers of excellence (SEV-2016-0683), MAT2015-69669-PM, ENE2013-49984-EXP, ENE2015-74009-JIN (co-funded by the European Regional Development Fund), and of the Spanish Science, Innovation and Universities: PGC2018-099744-B-100. F. R-M thanks the financial contribution of MIMECO through the program for young researchers support: TEC 2015 2015-74405-JIN. The authors greatly acknowledge the contribution of Prof. Francisco Meseguer for both the fruitful discussions and the revision of the manuscript, and Prof. Marie Louise McCarrey for careful proofreading of the manuscript.

References

1. Modest, M. F., *Radiative Heat Transfer*. Academic Press, New York: 2013.
2. Fernández-Hurtado, V.; Fernández-Domínguez, A. I.; Feist, J.; García-Vidal, F. J.; Cuevas, J. C., Super-Planckian far-field radiative heat transfer. *Phys. Rev. B* **2018,** *97*, 045408.
3. Cuevas, J. C., Thermal radiation from subwavelength objects and the violation of Planck's law. *Nat. Commun.* **2019,** *10*, 3342.
4. Hu, L.; Narayanaswamy, A.; Chen, X.; Chen, G., Near-field thermal radiation between two closely spaced glass plates exceeding Planck's blackbody radiation law. *Appl. Phys. Lett.* **2008,** *92*, 133106.
5. Thompson, D.; Zhu, L.; Mittapally, R.; Sadat, S.; Xing, Z.; McArdle, P.; Qazilbash, M. M.; Reddy, P.; Meyhofer, E., Hundred-fold enhancement in far-field radiative heat transfer over the blackbody limit. *Nature* **2018,** *561*, 216-221.
6. Wuttke, C.; Rauschenbeutel, A., Thermalization via Heat Radiation of an Individual Object Thinner than the Thermal Wavelength. *Phys. Rev. Lett.* **2013,** *111*, 024301.
7. Shin, S.; Elzouka, M.; Prasher, R.; Chen, R., Far-field coherent thermal emission from polaritonic resonance in individual anisotropic nanoribbons. *Nat. Commun.* **2019,** *10*, 1377.
8. Schuller, J. A.; Taubner, T.; Brongersma, M. L., Optical antenna thermal emitters. *Nat. Photonics* **2009,** *3*, 658-661.
9. Inoue, T.; De Zoysa, M.; Asano, T.; Noda, S., Realization of narrowband thermal emission with optical nanostructures. *Optica* **2015,** *2*, 27-35.
10. Li, W.; Fan, S., Nanophotonic control of thermal radiation for energy applications. *Opt. Express* **2018,** *26*, 15995-16021.
11. Greffet, J. J.; Carminati, R.; Joulain, K.; Mulet, J. P.; Mainguy, S.; Chen, Y., Coherent emission of light by thermal sources. *Nature* **2002,** *416* (6876), 61-4.
12. Lin, S. Y.; Fleming, J. G.; El-Kady, I., Three-dimensional photonic-crystal emission through thermal excitation. *Opt. Lett.* **2003,** *28* (20), 1909-11.

13. Chan, D. L.; Soljacic, M.; Joannopoulos, J. D., Thermal emission and design in 2D-periodic metallic photonic crystal slabs. *Opt. Express* **2006,** *14*, 8785-8796.
14. Garín, M.; Hernández, D.; Trifonov, T.; Alcubilla, R., Three-dimensional metallo-dielectric selective thermal emitters with high-temperature stability for thermophotovoltaic applications. *Sol. Energ. Mat. Sol. C.* **2015,** *134*, 22-28.
15. O'Regan, B. J.; Wang, Y.; Krauss, T. F., Silicon photonic crystal thermal emitter at near-infrared wavelengths. *Sci. Rep.* **2015,** *5*, 13415.
16. Wang, T.; peining, L.; C., D. N.; Giles, A. J.; Bezares, F. J.; Glembocki, O. J.; Caldwell, J. D.; Taubner, T., Phonon-Polaritonic Bowtie Nanoantennas: Controlling Infrared Thermal Radiation at the Nanoscale. *ACS Photonics* **2017,** *4*, 1753-1760.
17. Liu, X. T., T.; Starr, T.; F. Starr, A.; Jokerst, N.M.; Padilla, W. J., Taming the Blackbody with Infrared Metamaterials as Selective Thermal Emitters. *Phys. Rev. Lett.* **2011,** *107*, 045901.
18. Sakurai, A.; Yada, K.; Simomura, T.; Ju, S.; Kashiwagi, M.; Okada, H.; Nagao, T.; Tsuda, K.; Shiomi, J., Ultranarrow-Band Wavelength-Selective Thermal Emission with Aperiodic Multilayered Metamaterials by Bayesian Optimization. *ACS Cent. Sci.* **2019,** *5*, 319-326.
19. Miyazaki, H. T.; Ikeda, K.; Kasaya, T.; Yamamoto, K.; Inoue, Y.; Fujimura, K.; Kanakugi, T.; Okada, M.; Hatade, K., Thermal emission of two-color polarized infrared waves from integrated plasmon cavities. *Appl. Phys. Lett.* **2008,** *92*, 141114.
20. Ali, M. O.; Tait, N.; Gubta, S., High-Q all-dielectric thermal emitters for mid-infrared gas-sensing applications. *J. Opt. Soc. Am. A* **2018,** *35*, 119-124.
21. Meléndez, J.; de Castro, A. J.; López, F.; Meneses, J., Spectrally selective gas cell for electrooptical infrared compact multigas sensor. *Sensor Actuat. A-Phys* **1995,** *47*, 417-421.
22. Hildenbrand, J.; Korvink, J.; Wöllenstein, J.; Peter, C.; Kürzinger, A.; Naumann, F.; Ebert, M.; Lamprecht, F., Micromachined Mid-Infrared Emitter for Fast Transient Temperature Operation for Optical Gas Sensing Systems. *IEEE Sens. J.* **2010,** *10*, 353-362.
23. Inoue, T.; De Zoysa, M.; Asano, T.; Noda, S., Realization of dynamic thermal emission control. *Nat. Mater.* **2014,** *13* (10), 928-31.
24. Fenollosa, R.; Meseguer, F.; Tymczenko, M., Silicon Colloids: From Microcavities to Photonic Sponges. *Adv. Mater.* **2008,** *20*, 95-98.
25. Brace, D. B., *The Laws of Radiation and Absorption: Memoirs by Prévost, Stewart, Kirchhoff, and Kirchoff and Bunsen*. American Book Company: 1901.
26. Garin, M.; Fenollosa, R.; Ortega, P.; Meseguer, F., Light harvesting by a spherical silicon microcavity. *J. Appl. Phys.* **2016,** *119*, 033101.
27. Morino, R.; Tajima, H.; Sonoda, H.; Kobayashi, H.; Kanamoto, R.; Odashima, H.; Tachikawa, M., Mode-selective thermal radiation from a microsphere as a probe of optical properties of high-temperature materials. *Phys. Rev. A* **2017,** *95*, 063814.
28. Challener, W. A.; Peng, C.; Itagi, A. V.; Karns, D.; Peng, W.; Peng, Y.; Yang, X.; Zhu, X.; Gokemeijer, N. J.; Hsia, Y.-T.; Ju, G.; Rottmayer, R. E.; Seigler, M. A., Heat-assisted magnetic recording by a near-field transducer with efficient optical energy transfer. *Nat. Photonics* **2009,** *3*, 220-224.
29. Milichko, V. A.; Zuev, D. A.; Baranov, D. G.; Zograf, G. P.; Volodina, K.; Krasilin, A. A.; Mukhin, I. S.; Dmitriev, P. A.; Vinogradov, V. V.; Makarov, S. V.; Belov, P. A., Metal-Dielectric Nanocavity for Real-Time Tracing Molecular Events with Temperature Feedback. *Laser Photonics Rev.* **2018,** *12*, 1700227.
30. Iyer, S. S.; Xie, Y.-H., Light Emission from Silicon. *Science* **1993,** *260*, 40-48.

31. Pavesi, L., Silicon-Based Light Sources for Silicon Integrated Circuits. *Advances in Optical Technologies* **2008,** *2008*, 416926.
32. Garín, M.; Solà, M.; Julian, A.; Ortega, P., Enabling silicon-on-silicon photonics with pedestalled Mie resonators. *Nanoscale* **2018,** *10*, 14406-14413.
33. Fenollosa, R.; Garín, M.; Meseguer, F., Spherical silicon photonic microcavities: From amorphous to polycrystalline. *Phys. Rev. B* **2016,** *93*, 235307.
34. Shi, L.; Fenollosa, R.; Tuzer, T. U.; Meseguer, F., Angle-Dependent Quality Factor of Mie Resonances in Silicon-Colloid-Based Microcavities. *ACS Photonics* **2014,** *1*, 408-412.
35. Planck, M., *The Theory of Heat Radiation*. Dover Publication: 1912.
36. Kattawar, G. W.; Eisner, M., Radiation from a homogeneous isothermal sphere. *Appl. Optics* **1970,** *9* (12), 2685-90.
37. Bohren, C. F.; Huffman, D. R., *Absorption and Scattering of Light by Small Particles*. John Wiley & Sons: New York, 1998.
38. Sik, J.; Hora, J.; Humlícek, J., Optical functions of silicon at high temperatures. *Journal of Applied Physics* **1998,** *84*, 6291-6298.
39. Timans, P. J., Emissivity of silicon at elevated temperatures. *J. Appl. Phys.* **1993,** *74*, 6353-6364.
40. Rytov, S. M.; Kravtsov, Y. A.; Tatarskii, V. I., *Principles of Statistical Radiophysics*. Heidelberg, 1989; Vol. 3.
41. Sato, T., Spectral Emissivity of Silicon. *Jpn. J. Appl. Phys.* **1967,** *6*, 339-347.
42. Law, J. T., The High Temperature Oxidation of Silicon. *J. Phys. Chem.* **1957,** *61*, 1200-1205.

For Table of Contents Use Only

Thermal Emission of Silicon at Near Infrared Frequencies Mediated by Mie Resonances

Roberto Fenollosa, Fernando Ramiro-Manzano, Moisés Garín, and Ramón Alcubilla

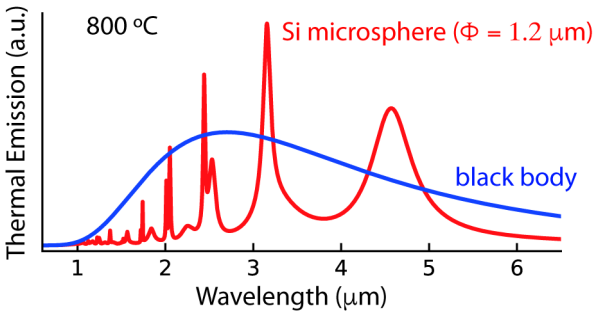

Calculated thermal emission of a black body and a 1.2 μm in diameter silicon micro-sphere